BJRS

BRAZILIAN JOURNAL
OF
RADIATION SCIENCES
10-03 (2022) 01-14

Dose reduction evaluation in radiosensitive tissues for head CT scans using two phantoms and bismuth eye shielding

Fernandes [a] L.C. and Mourão[a] A.P.

[a]*Departamento de Engenharia Nuclear, Universidade Federal de Minas Gerais*

Av. Presidente Antônio Carlos, 6627 - 31270-901 Belo Horizonte, MG

lorena.cfernandes@hotmail.com

ABSTRACT

Computed tomography is the imaging technique that most contributes to increasing the population average dose. The correct use of CT parameters such as load, voltage and pitch contribute to dose reduction in protocols. Dose reduction in the CT head protocol is important for protection of radiosensitive organs, such as the eye lenses and the thyroid. They receive significant doses when close to or in the irradiated field. The objective of this work is to present data on the variation of absorbed dose in the eye lenses and thyroid, with and without the use of bismuth eye shielding in head CT scans, and also to analyze the best dose-to-noise ratio in order to observe whether there is a decrease in image quality capable of rendering the proposed protocols useless. The method is based on head scans testing optimized protocols for the radiology service. Two male phantoms, one anthropomorphic and the other made in polymethyl methacrylate (PMMA), were used in the tests and radiochromic films were used to measure the absorbed dose values. The films were placed in the eye lenses and thyroid regions. Scans were performed on a GE CT scanner with 64-channel, Light Speed model. The obtained data allowed to observe the dose variation in the tissues and to conclude which of the evaluated protocols presented the best noise-to-dose ratio for the use of the bismuth eye shielding. The results showed for the protocol with the use of bismuth eye shielding a greater reduction of the absorbed dose in the thyroid, left eye lens and right eye lens, respectively, up to 49.4 %, 35.2 % and 31.1 % for the PMMA phantom and 62.7 %, 29.6 % and 12.8 % for the Alderson anthropomorphic phantom. A variation in noise was obtained between the images with and without bismuth shielding of up to 0.16% for the Alderson anthropomorphic phantom and 0.13 % for the PMMA phantom.

Keywords: **Computed tomography, bismuth eye shielding, dosimetry, radiochromic film.**

ISSN: 2319-0612
DOI: https://doi.org/10.15392/bjrs.v10i3.2040
Submitted: 2022-03-21
Accepted: 2022-07-04

1. INTRODUCTION

Advances in Computed Tomography (CT) technology have contributed to the increase in the number of CT scans, and consequently the average dose per person has increased [1].

Cohort's study on cataract generation related to low doses of ionizing radiation showed evidence that low doses can cause damage to the lens or even cataract formation in the long term [3]. Yuan, et al., 2012, presented in their study that various exposures to head and neck CT scan increased risk of cataract [4]. The National Council on Radiation Protection and Measurements (NCRP) suggests that cataract formation has no apparent threshold, with its chances of occurring probabilistically increasing as the radiation dose increases [5].

Another radiosensitive organ that should be given importance in head and neck exams is the thyroid gland [6,7]. Tipnis et al., 2015, estimated to young patients (≤20 years) have high risk developing thyroid cancer at doses above 50 mGy, in neck CT scans [8].

However, it is important to practice the ALARA principle (as low as reasonably possible) on CT scans. Currently, recent technologies prioritize dose reduction in sensitive organs, maintaining diagnostic image quality, such as: tube current modulation, tube inclination, bismuth shielding, and iterative reconstruction of the 3D image. Since the use of bismuth shielding requires less expense and can be applied to various types of CT scans, it is an effective alternative for protecting the patient's eyes and thyroid [9, 10].

Studies suggest the use of eye shielding, bismuth or barium material, to obtain head images in CT and to reduce the radiation doses in the eye lenses. The radiation induces the eye lens opacification and cataract. Dose reduction in head CT scans is especially important for patients with chronic diseases, who are frequently exposed to radiation, for example hydrocephalus, about 26% of patients receive radiation doses in the eye region greater than 150 mSv in 3 years [11, 12, 13, 14].

The use of the bismuth shielding can contribute to the generation of noise and artifacts in the image, due to the hardening of the radiation beam in the region of the protector [15]. To reduce this type of interference, these protections must be used correctly.

The other study points out that bismuth protectors are an effective instrument for dose reduction in the eyes, but on the other hand there was an increase in the noise level over the brain regions (anterior, middle and posterior cranial zones) [16]. Salinas, et al. concludes that one of the ways to

improve its use is by obtaining appropriate design dedicated protection only for each eye, which generates less artifacts than traditional protection model [17].

In this sense, the objective of this work was to estimate organ absorbed doses in the thyroid and the eye lenses, and the image noise due to CT head scans, using a PMMA and an anthropomorphic phantom with and without bismuth eye shields.

2. MATERIALS AND METHODS

The following materials were used: GE Light Speed VCT scanner with 64-channels; Two PMMA phantoms, cylinders of 16 and 11 cm in diameter representing respectively the head and the neck; an anthropomorphic Alderson male phantom with an average head diameter of 17.9 cm (20.1 cm on the long axis and 15.7 cm on the short axis); the radiochromic films Gafchromic XRQA2 [18], a scanner HP Photosmart C4480; an ionization pencil chamber Accu-Gold model 10X6-0.6CT; and a bismuth eye shielding by Biosmith, model AttenuRad CT Eye Shield, with dimensions: 14 cm wide, 3 cm high and 0.1 cm thick [19].

2.1. Eye lens and thyroid dose measurements with and without bismuth eye shielding

For dose measurement in the eye lenses (left and right) and thyroid, the head PMMA and the anthropomorphic phantoms were positioned in the isocenter of the CT scanner. The phantoms were placed juxtaposed using a head support for better stabilization of the phantoms during the table displacement.

The bismuth shielding was placed on the surface of the eyes' region, for both phantoms, to perform head CT scans. Figure 1 shows in (a) the PMMA head phantom and in (b) the anthropomorphic phantom using the bismuth shielding on the eyes.

Two different phantoms were used to compare the absorbed dose data and analyze the limitation of the phantoms for practical application. The absorbed dose will be analyzed for only one bismuth eye shielding thickness, because it was implanted together with the optimized protocols.

Figure 1: *Positioning of the phantoms in the CT scanner with bismuth eye shielding. (a) PMMA head phantom and (b) anthropomorphic phantom.*

In this paper the radiochromic film that was cut in strips with 2 x 0.5 cm^2. The radiochromic films were placed on the outside of the phantoms, in the position's right eye lens, left eye lens and thyroid. The phantoms were scanned, with and without the bismuth eye shielding, using three different head CT protocols, in helical mode using a pitch of 0.984, tube time of 1.0 s, image reconstruction of 5 mm, scanning distance of 10 cm. The variable parameters of the acquisition protocols were the voltage (kV) and the tube current (mA). Both phantoms were used to perform head CT scans.

Digital images of the radiochromic films strips were obtained before and 24 h after the irradiation. Film strips images were generated in a scanner in reflective mode.

Three optimized protocols were tested: two using the low tube voltages (80 kV and 100 kV) and one standard tube voltage (120 kV). Current values chosen for the dosimetry tests were previously tested according to the CT scanner possibilities in order to keep the noise around 1% by system Automatic Exposition Control (AEC). The value of voltage and current used in the tested protocols are in Table 1.

Table 1: Variable parameters of acquisition protocols

Parameter	Protocol 1	Protocol 2	Protocol 3
Voltage (kV)	80	100	120
Current (mA)	135	75	50

In order to compare eye lenses and thyroid doses using the PMMA phantom, the same methodology was performed with the male Alderson anthropomorphic phantom.

From the experiments performed with the PMMA and anthropomorphic Alderson phantoms, with and without the bismuth eye shielding, the images were obtained for each protocol. The irradiated radiochromic films were digitized and the gray values were read using the ImageJ software [18, 20].

The calibration of the radiochromic film was performed at CT with the ionization chamber [21, 22]. To ionization chamber was realized standard measures. They were obtained to voltages of 80, 100 and 120 kV, and set tube parameters for current (200 mA), tube rotation time (0.5 s), and slice thickness (10 mm). Kerma measurements from the scans were repeated five times for each PMMA phantom openings. The air kerma value of Table 1 was obtained using equation 1.

$$k = k_{\mathrm{c}} \frac{C_0}{C_{\mathrm{c}}} \tag{1}$$

Since k is the new air kerma value (converted to the optimized charge range), kc is the air kerma measured with the ionization chamber, C_0 is the charge to each protocol of Table 1, C_{c} is the charge used for measurements with the chamber.

The calibration coefficients of the radiochromic film were obtained for each protocol, relating the gray scale of the irradiated film and the air kerma value of equation 1.

The air kerma values were converted into an absorbed dose for both phantoms. An average of the absorbed dose values of the radiochromic film was performed.

2.2. Image noise analysis

Images were evaluated using the RadiAnt DICOM Viewer software [23]. In the PMMA head phantom, the noise was analyzed in the central slice images. It was selected a region of interest (ROI) of 1 cm². From the standard deviation and the intensity average values obtained, the noise value for each protocol was calculated using the equation 2.

For the Alderson phantom, the noise of the central slice of the phantom through an ROI with an area of 1 cm² in a uniform region of the brain was studied. The noise was calculated from equation 2 [24].

$$R = \frac{\sigma}{M + 1000} \quad (2)$$

where R is the image noise, σ is the standard deviation of the CT numbers, and M is the average value on the Hounsfield scale.

3. RESULTS AND DISCUSSION

The factors used for converting air kerma into an absorbed dose in the PMMA were: 1.0106, 1.0324, 1.0418 for respectively for average energy of 80, 100, 120 kV [25].

The radiochromic films calibration presented an expanded uncertainty of 4.73% with a confidence level of approximately 95.5%, and the ionization chamber with the expanded uncertainty of 4.035% with a confidence level of approximately 95.5%.

3.1. Dose and image evaluation using PMMA phantoms

The left eye lens, right eye lens and thyroid dose results of protocols (1, 2 and 3) with and without bismuth eye shielding in the PMMA phantom are presented in the Table 2.

Table 2: Absorbed dose (mGy) for the PMMA phantoms with respective standard deviation.

Organ	Shielding	Protocol 1	Protocol 2	Protocol 3
Thyroid	With	1.55 ± 0.11	1.70 ± 0.25	1.27 ± 0.17
	Without	3.06 ± 0.15	2.01 ± 0.21	1.55 ± 0.18
Left eye lens	With	6.17 ± 0.29	8.01 ± 0.19	6.72 ± 0.35
	Without	9.53 ± 0.28	11.80 ± 0.25	9.75 ± 0.24
Right eye lens	With	7.43 ± 0.25	8.94 ± 0.25	8.04 ± 0.38
	Without	9.90 ± 0.11	12.16 ± 0.26	9.84 ± 0.29

Table 2 data shows the efficiency in the use of bismuth eye shielding. When the shielding was used, the dose was decreased in the left and right eye lens and thyroid, when compared to scanning without bismuth eye shielding.

It was found that the greatest dose reduction occurred for protocol 1, with a percentage reduction of 49.4 % in the thyroid, 35.2 % in the left lens and 24.9 % in the right lens. For protocol 2, the reduction was 15.1 %, 32.1 % and 26.46 % in the thyroid, left lens and right lens, respectively; and in protocol 3, 17.9 %, 18.9 % and 31.1 %.

With the data in Table 2, it is possible to verify that the lowest dose protocol in the organs under study is the protocol 3. It is observed that the reduction of the doses with the use of the bismuth eye shielding is a rule.

Note that protocol 3 has a lower dose than protocol 2, this is because its current is lower and the penetration of the 120 kV beam is greater in the phantom, thus reducing the dose on the phantom surface.

Table 3 presents the percentage noise values found from the used protocols, with and without bismuth eye shielding, and the difference in percentage. These values were recorded from the central slice image.

Table 3: Image noise values from protocols 1, 2 and 3 using PMMA phantoms.

Shielding	**Protocol 1**	**Protocol 2**	**Protocol 3**
with	0.89 %	0.86 %	0.84 %
without	0.87 %	0.72 %	0.73 %
Variation	0.02 %	0.13 %	0.11 %

Table 3 shows that there was an increase in noise values in the central slice with the use of bismuth eye shielding. The highest noise value was from protocol 1, but it was less than 1 %, considering the noise value ≤ 1 % acceptable [26].

3.2. Dose values and image evaluation using Alderson anthropomorphic phantom

The dose results in the left and right eye lens and thyroid for protocols 1, 2 and 3 with and without the bismuth eye shielding in the Alderson anthropomorphic phantom are presented in Table 4.

Table 4: Absorbed dose (mGy) for the Alderson anthropomorphic phantom with standard deviation.

Organ	Shielding	Protocol 1	Protocol 2	Protocol 3
Thyroid	With	0.79 ± 0.17	0.87 ± 0.18	1.40 ± 0.13
	Without	2.14 ± 0.21	1.77 ± 0.14	2.02 ±0.19
Left eye lens	With	6.68 ± 0.22	7.99 ± 0.33	7.83 ± 0.12
	Without	9.04 ± 0.17	11.35 ± 0.25	9.48 ±0.29
Right eye lens	With	8.16 ± 0.27	9.54 ± 0.38	7.39 ± 0.18
	Without	9.36 ± 0.18	10.51 ± 0.26	8.28 ± 0.24

In protocols 1, 2 and 3, the use of the shielding contributed to the reduction of the dose in the thyroid and left and right lens, and respectively had a reduction: in protocol 1 of 62.7 %, 26.1 % and 12.8 %, for protocol 2 with 50.5 %, 29.6 % and 9.2 %, and for protocol 3 with 30.6 %, 17.4 % and 10.7 %.

Table 5 presents the noise data from the protocols 1, 2 and 3 images using the Alderson anthropomorphic phantom. Since the noise of the central slice with the use of bismuth shielding, in protocol 1, presented greater than 1 %, and the one without shielding is in the noise range threshold for good diagnosis. For the other protocols, 2 and 3, the noise for both regions were lower than 1%, and the difference for these showed not so much degradation in the image.

Table 5: Image noise data from protocols 1, 2 and 3 using Alderson anthropomorphic phantom

Shielding	Protocol 1	Protocol 2	Protocol 3
with	1.16 %	0.91 %	0.73 %
without	1 %	0.80 %	0.72 %
Variation	0.16 %	0.11 %	0.01 %

3.3. Evaluation dose profile of PMMA and anthropomorphic Alderson phantoms

The eye lenses dose profiles of the protocols 1, 2 and 3 are presented respectively in Figure 2, 3 and 4. In these figures, it is possible to observe the variation of the dose deposition along the right and left lens for both studied phantoms. Note that the absorbed dose variation curve has lower values in the anthropomorphic Alderson phantom when compared to the PMMA Phantom, this is due to the different head size and material.

It was noticed, in common, in the central region of Figures 2, 3 and 4, that the spectrum of the right eye lens with PMMA phantom and shielding and the left eye lens without shielding in the anthropomorphic Alderson phantom have very close dose variations.

Figure 2: *PMMA and anthropomorphic Alderson phantom lenses dose profile of protocol 1.*

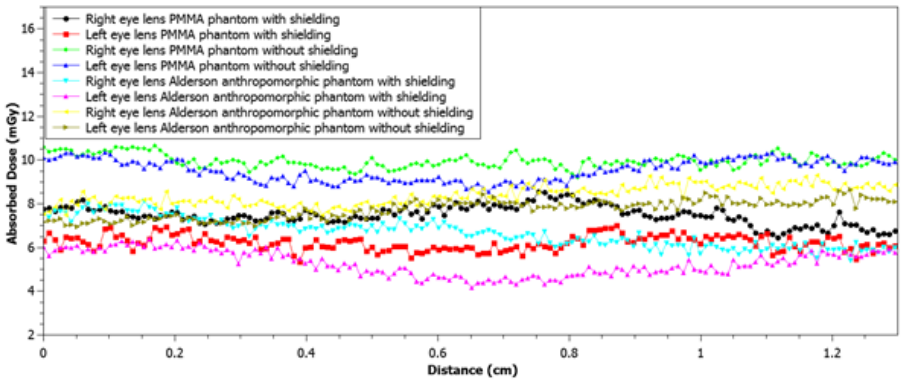

Figure 3: *PMMA and anthropomorphic Alderson phantom lenses dose profile of protocol 2.*

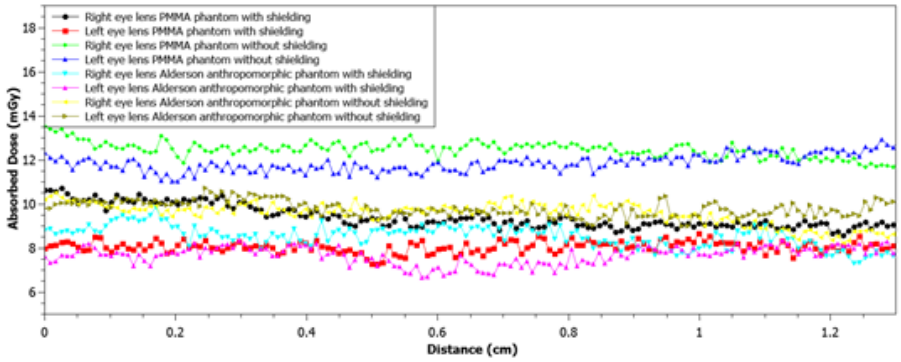

Figure 4: *PMMA and anthropomorphic Alderson phantom lenses dose profile of protocol 3.*

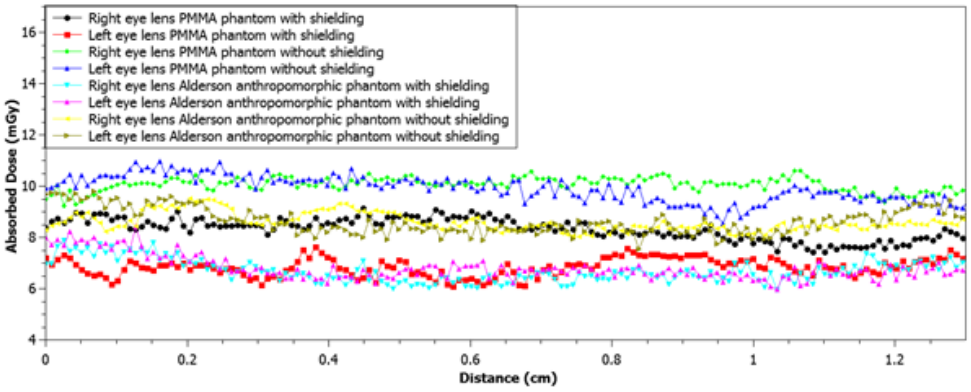

CT scan with AEC systems control the current output of the X-ray tube according to the image noise level selected by the user. The system scans with low energy to be able to recognize the structures arranged in the field to be irradiated. But when the system is faced with a material with a high atomic number, the system increases the number of photons in that region to maintain the quality of the selected image, as a consequence the dose will be increased [27].

In this sense, the methodology used in this work reduced the radiation exposure of superficial radiosensitive organs, such as the eye lenses and the thyroid. Since it was possible to use the AEC and eye shielding, acquired in independent tests, in order to reduce the dose in the eye region.

It was observed that with both methods of evaluating the use of the bismuth eye shielding, described in this work, the diagnostic image of the brain tissue did not show a significant increase in noise when compared to the protocol without the bismuth shielding. The image quality was maintained as long as there was a significant reduction in the dose of the lens. In consideration, the bismuth shielding has a good attenuation of low-energy photons, which tend to deposit on the surface of the phantom [14].

An accumulated dose in the eyes contributes to an increase in the rate of opacification and aging of the lens. One of the ways to delay these eye diseases is to propose the bismuth protector together with optimized protocols [4, 13].

According with recent publications, to dose in head computed tomography between 91.11–103.63 mGy was estimated the excess relative risk (ERR) of 0.03 to the generation of cataracts. A linear approximation was made between the incidence of cataracts and the cumulative dose of gamma rays

received by occupationally exposed workers in Mayak, with an estimated ERR of 0.28 per Gy [12, 28].

Therefore, in the protocol 3 there was absorbed dose reduction in the eye lens using bismuth eye shielding. With this protocol, the cataract induction risks were reduced in 17.4% and 10.7% for the left and right eyes, respectively.

4. CONCLUSION

The PMMA and anthropomorphic Alderson phantoms differ in the composition of the material as well as in their dimensions. The PMMA phantom, due to its low cost and easy handling, is more used in practice. However, the Alderson anthropomorphic phantom has material properties and dimensions similar to a standard human body.

In this work, the difference between the absorbed doses and noise of each protocol proposed for each phantom was observed. But in general, for both there was an effectiveness of the dose reduction for the use of bismuth eye shielding.

In the suggested protocols, the noise values in the Alderson phantom was higher than in the PMMA phantom for protocol 1 and 3 and similar for protocol 2. With a difference of 0.13 %, 0.08 % and 0.01 % without bismuth eye shielding, and 0.27 %, 0.05 % and 0.11 % with bismuth eye shielding, for protocols 1, 2 and 3 respectively.

The protocol for the greatest reduction of the absorbed dose, with the use of bismuth eye shielding, in the eyes lens and thyroid was protocol 1, but its noise value was higher than the stipulated 1% for the Alderson Anthropormofic phantom. However, protocol 3 obtained the lowest noise for both phantoms and also a reduction in the absorbed dose when using the bismuth protector.

ACKNOWLEDGMENT

The authors are grateful to the Coordenação de Aperfeiçoamento de Pessoal de Nível Superior (CAPES), the Fundação de Amparo à Pesquisa do Estado de Minas Gerais (FAPEMIG), the Centro de Imagem Molecular do INCT-MM Faculdade de Medicina da Universidade Federal de Minas Gerais, and the Centro de Desenvolvimento da Tecnologia Nuclear

REFERENCES

[1] Thurston, Jim. NCRP Report No. 160: ionizing radiation exposure of the population of the United States. 2010.

[2] ICRP. **The 2007 Recommendations of the International Commission on Radiological Protection**. **ICRP Publication 103 (2007).** Ann. ICRP, Volume 37, p. 1-332.

[3] CHODICK, G. et al. Risk of cataract after exposure to low doses of ionizing radiation: a 20-year prospective cohort study among US radiologic technologists. **American journal of epidemiology**, v. 168, n. 6, p. 620-631, 2008.

[4] YUAN, Mei-Kang et al. The risk of cataract associated with repeated head and neck CT studies: a nationwide population-based study. **American Journal of Roentgenology**, v. 201, n. 3, p. 626-630, 2013.

[5] National Council on Radiation Protection and Measurements. **Guidance on Radiation Dose Limits for the Lens of the Eye, NCRP Commentary No. 26.** National Council on Radiation Protection and Measurements, Bethesda, Maryland, 2016.

[6] SCHONFELD, S. J.; LEE, C.; DE GONZALEZ, A. B.. Medical exposure to radiation and thyroid cancer. **Clinical Oncology**, v. 23, n. 4, p. 244-250, 2011.

[7] Baker, Stephen R.; BHATTI, Waseem A. The thyroid cancer epidemic: is it the dark side of the CT revolution?. **European journal of radiology,** v. 60, n. 1, p. 67-69, 2006.

[8] TIPNIS, S. V. et al. Thyroid doses and risks to adult patients undergoing neck CT examinations. **American Journal of Roentgenology**, v. 204, n. 5, p. 1064-1068, 2015.

[9] CIARMATORI, A. et al. Reducing absorbed dose to eye lenses in head CT examinations: the effect of bismuth shielding. **Australasian physical & engineering sciences in medicine,** v. 39, n. 2, p. 583-589, 2016.

[10] OMER, Hiba et al. Eye lens and thyroid gland radiation exposure for patients undergoing brain computed tomography examination. **Saudi Journal of Biological Sciences,** v. 28, n. 1, p. 342-346, 2021.

[11] International Atomic Energy Agency (IAEA). Radiation and cataract: staff protection. Available at: <https://www.iaea.org/resources/rpop/health-professionals/radiology/cataract/patients> Last accessed: 19 Nov. 2020.

[12] LIN, Ming-Fang et al. Topogram-based tube current modulation of head computed tomography for optimizing image quality while protecting the eye lens with shielding. **Acta Radiologica**, v. 60, n. 1, p. 61-67, 2019.

[13] LEE, Jong-Woong; KWEON, Dae Cheol. Assessment of dose reduction and image quality by barium composite shielding in head and chest CT. **Radiation Effects and Defects in Solids**, p. 1-18, 2020.

[14] BANGASSI, T. N. K.; SAMBA, O. N.; THIERENS, H.; BACHER, K. Eye Lens Dose Reduction in Head CT Using Bismuth Shielding: Application in CT Facility in Cameroon. **AASCIT Journal of Health**, vol.5,nº1. pg 11-15, 2018.

[15] Radiopaedia. Beam hardening. Available at: <https://radiopaedia.org/articles/beam-hardening> Last accessed: 19 Nov. 2020.

[16] LAI, C. W. K. et al. Reducing the radiation dose to the eye lens region during CT brain examination: the potential beneficial effect of the combined use of bolus and a bismuth shield. **Radioprotection**, v. 50, n. 3, p. 195-201, 2015.

[17] SALINAS, C. Leiva et al. Bismuth shielding at head CT: Impact of a novel design on the image quality and dose reduction to the lens. **ECR 2015**, 2015.

[18] GIADDUI, T. et al. Characteristics of Gafchromic XRQA2 films for kV image dose measurement. **Medical physics**, v. 39, n. 2, p. 842-850, 2012.

[19] BioSmith. Eye shield. Available at: < https://www.fandlmedicalproducts.com/AttenuRad-CT-Eye-Shield.html > Last accessed: 19 Jan. 2021.

[20] RASBAND, W. S. **ImageJ, U. S. National Institutes of Health**. Bethesda, Maryland, USA. 2011. Available at: <http://imagej.nih.gov/ij/>. Last accessed: 19 Nov. 2020.

[21] MOURÃO, A. P.; ALONSO, T. C.; DASILVA, T. A. Dose profile variation with voltage in head CT scans using radiochromic films. **Radiation Physics and Chemistry**, v. 95, p. 254-257, 2014.

[22] RAMPADO, O.; GARELLI, E.; ROPOLO, R. Computed tomography dose measurements with radiochromic films and a flatbed scanner. **Medical physics**, v. 37, n. 1, p. 189-196, 2010.

[23] RadiAnt DICOM Viewer. Available at: <https://www.radiantviewer.com/dicom-viewer-manual/>. Last accessed: 19 Nov. 2020.

[24] MOURÃO, Arnaldo Prata. **Tomografia computadorizada: tecnologias e aplicações**. Difusão Editora, 2018.

[25] NIST—National Institute of Standards and Technology. Available at: < https://www.nist.gov/national-institute-standards-and-technology > Last accessed: 19 Jan. 2020.

[26] DALMAZO, J. et al. Radiation dose optimization in routine computed tomography: a study of feasibility in a University Hospital. **Radiologia Brasileira**, v. 43, p. 241-248, 2010.

[27] American Association of Physicists in Medicine. AAPM position statement on the use of bismuth shielding for the purpose of dose reduction in CT scanning. **AAPM website**., 2012. Available at: <https://www.aapm.org/publicgeneral/bismuthshielding.pdf>. Last accessed: 19 Nov. 2020.

[28] HAMADA, Nobuyuki. Ionizing radiation sensitivity of the ocular lens and its dose rate dependence. **International Journal of Radiation Biology**, v. 93, n. 10, p. 1024-1034, 2017.